Core-breakup reactions of the halo muclei ^{11}Be and ^{11}Li: momentum distributions and shadow effects

S. Grevy, L. Axelsson, J.C. Angélique, R. Anne, D. Guillemaud-Mueller, P G. Hansen, P. Hornshoj, B. Jonson, M. Lewitowicz, a C. Mueller, et al.

LABORATOIRE
DE
PHYSIQUE CORPUSCULAI

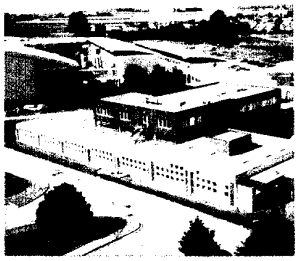

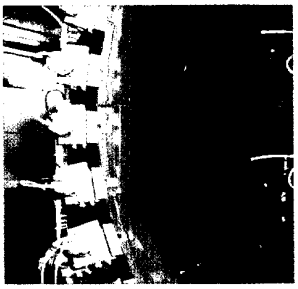

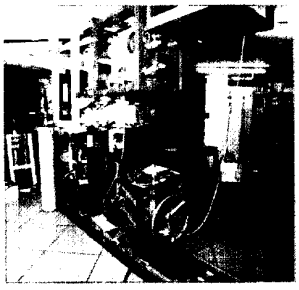

Core-breakup reactions of the halo nuclei ^{11}Be and ^{11}Li: momentum distributions and shadow effects

S. Grévy, L. Axelsson, J.C. Angélique, R. Anne, D. Guillemaud-Mueller, P.G. Hansen, P. Hornshøj, B. Jonson, M. Lewitowicz, A.C. Mueller, T. Nilsson, G. Nyman, N.A. Orr, F. Pougheon, K. Riisager, M.-G. Saint-Laurent, M. Smedberg, O. Sorlin

March 1999 LPCC 99-12

Nuclear Physics A 650 (1999) 47-61

CENTRE NATIONAL DE LA RECHERCHE SCIENTIFIQUE

INSTITUT NATIONAL
DE PHYSIQUE NUCLÉAIRE ET DE PHYSIQUE DES PARTICULES

INSTITUT DES SCIENCES DE LA MATIÈRE ET DU RAYONNEMENT

UNIVERSITÉ DE CAEN

- U.M.R.6534 -
ISMRA - 6, Boulevard Maréchal Juin - 14050 CAEN CEDEX - FRANCE

Téléphone : 02 31 45 25 00 - Télécopie : 02 31 45 25 49
Internet : http://caeinfo.in2p3.fr

CNRS CENTRE NATIONAL DE LA RECHERCHE SCIENTIFIQUE IN2P3 ISMRA

Nuclear Physics A 650 (1999) 47–61

Core-breakup reactions of the halo nuclei ^{11}Be and ^{11}Li: momentum distributions and shadow effects

S. Grévy[a,1], L. Axelsson[b], J.C. Angélique[c], R. Anne[d], D. Guillemaud-Mueller[a], P. G. Hansen[e], P. Hornshøj[f], B. Jonson[b], M. Lewitowicz[d], A.C. Mueller[a], T. Nilsson[b,2], G. Nyman[b], N.A. Orr[c], F. Pougheon[a], K. Riisager[f], M.-G. Saint-Laurent[d], M. Smedberg[b], O. Sorlin[a]

[a] *Institut de Physique Nucléaire, IN2P3-CNRS, F-91406 Orsay Cedex, France*
[b] *Fysiska Institutionen, Chalmers Tekniska Högskola, S-41296 Gothenburg, Sweden*
[c] *Laboratoire de Physique Corpusculaire, IN2P3-CNRS, ISMRA, F-14050 Caen Cedex, France*
[d] *Grand Accélérateur National d'Ions Lourds, F-14021 Caen Cedex, France*
[e] *National Superconducting Cyclotron Laboratory, Michigan State University, East Lansing, MI 48824, USA*
[f] *Institut for Fysik og Astronomi, Aarhus Universitet, DK-8000 Aarhus C, Denmark*

Received 25 November 1998; revised 26 January 1999; accepted 15 February 1999

Abstract

The halo nuclei ^{11}Be and ^{11}Li have been studied in core-breakup reactions where the halo neutrons are expected to be released without a major distortion due to the reaction. The widths of the halo-neutron momentum distributions have been extracted in coincidence with He fragments, $\Gamma = 32 \pm 4$ MeV/c, and Li fragments, $\Gamma = 42 \pm 4$ MeV/c for ^{11}Be and with He fragments, $\Gamma = 42 \pm 6$ MeV/c for ^{11}Li. The ^{11}Be breakup gives a very low neutron multiplicity of 0.38 ± 0.09 which is a manifestation of the shadowing of the neutron in the core-breakup reaction. This value can be understood from a simple theoretical calculation, which also accounts for the observed transverse momentum widths at small angles. © 1999 Elsevier Science B.V.

PACS: 21.10.Gv; 25.60.Gc; 27.20.+n
Keywords: Radioactive beams; Halo nuclei; Core-breakup reactions; Momentum widths; Shadowing

[1] Permanent address: LPC, IN2P3-CNRS, ISMRA, F-14050 Caen Cedex, France.
[2] Current address: EP division, CERN, CH-1211 Geneva 23, Switzerland.

PII S0375-9474(99)00102-5

1. Introduction

A number of methods for studying the structure of halo nuclei through breakup reactions have been proposed and tested during the last decade [1–3]. This paper describes a careful study of one of these processes, the core-breakup reaction [4,5]. The motivation for studying this process can be stated briefly as follows: Assume that a halo nucleus is well described as a core and a loosely bound halo. For a sufficiently fast reaction, i.e. at beam velocities large compared to internal motion in the halo, one might hope that the halo-particles will be only slightly perturbed in reactions that breakup the core. A test of this idea should (i) find evidence supporting the two-component picture (core + halo), (ii) identify the core and halo components separately and (iii) check for effects due to the reaction mechanism. Furthermore the test should be performed on nuclei with a good and well-established halo structure. Two prime examples are ^{11}Be and ^{11}Li, the best-studied one- and two-neutron halo nuclei, respectively. The core-breakup reaction has been briefly studied for these two nuclei earlier [4,5] and indications for a two component structure were seen in the neutron momentum distributions.

The aim of the present work is to provide better data for the angular distribution of fast neutrons emerging from core-breakup reactions in order to enable more stringent tests to be performed. Specifically, for both studied halo nuclei we have carried out the "corresponding" reaction experiments involving only the core nucleus, i.e. ^{10}Be and ^{9}Li, respectively. These reactions should yield a pure core component and thus answer to point (ii). Concerning point (iii), it is well established [1] that the reaction mechanism can have a major effect in dissociation reactions in which the core survives. We expect collisions that breakup the core to take place at small impact parameters and on a short time scale, so that the sudden approximation might be applicable for the halo neutrons. However, we can still have indirect effects partly from final state interactions (FSI), partly from shadowing. Effects from FSI can occur if the neutron + core-fragment system has strong resonances at sufficiently low energy [6–8]. Since core-breakup reactions are more violent than dissociation reactions one can hope FSI will be of less importance. Shadowing, the modification of the momentum distribution due to halo neutrons reacting during the collisions [9–11], will definitely enter. This will be discussed in detail.

The core-breakup reactions of ^{11}Be and ^{11}Li have already been studied in previous experiments. In the first one performed at GANIL, a beam of ^{11}Be with an energy of 41 MeV/u was used and all events except those from dissociation reactions were studied (referred to as *restricted inclusive* channel [4] meaning "single neutron plus anything different from ^{10}Be"). This selection is less restrictive than ours since, in the present study, the halo neutrons were selected in coincidence with a fragment of lower charge than the core, the channels we shall be looking at are thus distinguished by fragment Z. Such a selection is important if some reactions are influenced by FSI, thereby giving a different distribution. Moreover, the neutrons coming from the core fragmentation of ^{10}Be were not removed in that experiment. The results show identical angular distributions from Be and Ti targets and were consistent with a superposition

of a narrow and a broad component. In the second experiment performed at GSI with a ^{11}Be beam of 460 MeV/u on a C target by Nilsson et al. [5] in which ^{7,8}Li were selected in the exit channel, the contribution of neutrons from ^{10}Be breakup was not subtracted either. These studies lead to an average value for the width of the momentum distributions of neutrons from ^{11}Be of 60±5 MeV/c [5].

At GANIL the core-breakup channel from ^{11}Li was studied with a beam of 28 MeV/u on a Be target and only a rough subtraction of the ^{9}Li contribution could be done. Another experiment was performed at GSI with a 280 MeV/u ^{11}Li beam on a C target, where the acceptance was limited to fragments with $A/Z \geqslant 2.3$. The contribution of neutrons from ^{9}Li breakup was not subtracted. The widths obtained in these studies from the neutron momentum distributions are consistent with an average value of 41±4 MeV/c [5].

More recently, core-breakup reactions were used by Marqués et al. [12] in the study of the expected one-neutron halo nucleus ^{19}C. The background of the neutrons coming from the breakup of ^{18}C was not measured but estimated from the distribution of ^{24}F. Due to this and the low statistics, the width has been extracted with a relatively large error (55±16 MeV/c). This result overlaps two conflicting values obtained from the parallel momentum distribution of the core ^{18}C in dissociation reactions (42±4 MeV/c at MSU at 88 MeV/u [13] and 69±3 MeV/c at GSI at 914 MeV/u [14]). This confirms the importance of a proper subtraction of the background and a restrictive selection in the exit channel.

2. Experimental setup

The present experiment was performed at GANIL. The LISE3 spectrometer [15] was used to extract an almost pure secondary beam produced by fragmentation of an ^{18}O primary beam with an energy of 76 MeV/u. A 2 mm Be and a 6 mm C target were used in the production of the Be and Li isotopes, respectively. To purify the secondary beams, an achromatic degrader of Al (average thickness of 1100 μm) was mounted in the intermediate focal plane between the two dipole magnets. At the end of LISE3, the beams, whose impurities were less than 10^{-3}, were focused onto a reaction target consisting of Be (2000 μm) and placed inside a detector telescope, see inset in Fig. 1. The telescope consisted of two thin Si detectors (300 μm) and a thick CsI detector (4500 μm), where the first detector started the time of flight. In order to minimize scattering and absorption of neutrons, the reaction chamber was equipped with a thin (500 μm) exit window of stainless steel.

In the middle of the target, the energies of the ^{11}Li and ^{11}Be beams were 29.9 MeV/u and 38.5 MeV/u, respectively. In order to estimate and subtract the contribution of neutrons coming from the core, measurements with beams of the core nuclei (^{9}Li and ^{10}Be), with the same energy in the middle of the target as the corresponding halo nucleus, were performed. The background arising from the telescope was measured without target in an energy condition corresponding to the energy loss in the reaction

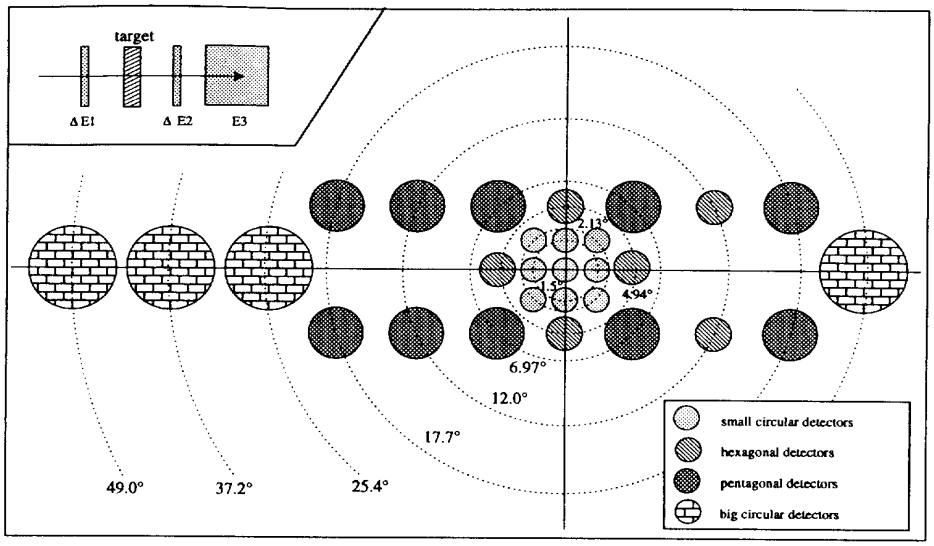

Fig. 1. Geometry of the experimental setup for the detection of neutrons in a wall of 29 liquid-scintillator detectors of varying sizes. In upper left, the telescope for the detection of heavy ions placed in vacuum in the reaction chamber at the end of the LISE3 spectrometer is shown.

target.

Fast neutrons from the breakup reactions were detected with a setup similar to that used in Refs. [4,16] but with a modified configuration giving higher granularity at small angles, see Fig. 1. The array of 29 neutron detectors was placed at a distance of 3 m behind the reaction target covering angles from $-25°$ to $53°$ around the direction of the incoming beam. The energy and momentum of the neutrons were calculated from the time-of-flight between the first ΔE detector and the neutron detectors.

3. Analysis and results

3.1. Charged fragments

As mentioned earlier, the selections of fragments in this experiment were more restrictive than in general core-breakup measurements by accepting only Li or He fragments. A heavy-ion identification plot containing fragments from ^{11}Be reacting in the target, in coincidence with a neutron, is shown in Fig. 2, including selections used in the analysis. It is important to note that all reactions giving one (or two) alpha particles are kinematically separated by their residual energy from the ones giving a Li charged fragment. The same selections as were used for the halo nuclei were also used for ^{10}Be and ^{9}Li to estimate the contribution of neutrons arising from breakup of the core in the ^{11}Be and ^{11}Li distributions. Measurements without target showed that the background

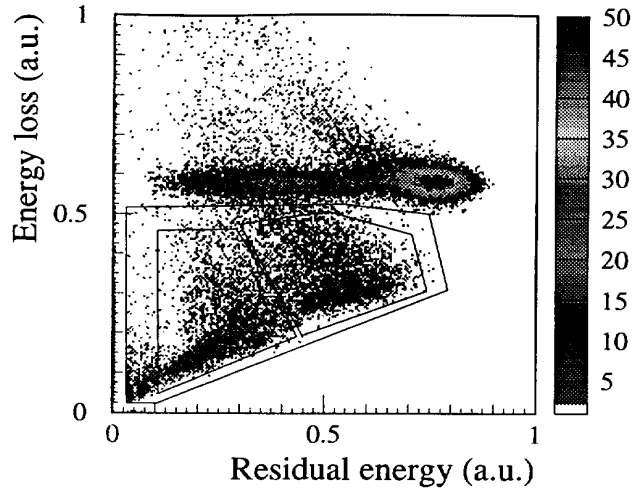

Fig. 2. Identification plot (ΔE vs. E_{residual}, a.u. = arbitrary units) for fragments arising from the ^{11}Be reactions in the Be target. The small cuts on the right and on the left represents the Li and He isotopes respectively whereas the larger represents all the events with a charge inferior to that of the projectile.

Table 1
Cross sections for ^{11}Be and ^{10}Be in coincidence with Li and He fragments and for ^{11}Li and ^{9}Li in coincidence with He fragments. All values are for a Be target

Beam	σ_r (mb)	
	He fragments	Li fragments
^{11}Be	125±20	245±25
^{10}Be	135±15	260±25
^{11}Li	180±25	-
^{9}Li	190±25	-

due to reactions in the detectors was negligible and was therefore not considered in the analysis. The cross sections from the breakup reactions in the Be target are obtained for each secondary beam (Table 1) in the same way as in previous papers [4] using Eq. (1). N_i and N_d are respectively the number of incident and detected events, A and d are the mass number and the thickness of the target whereas $\mathcal{N}_a$ and ϵ are respectively the Avogadro number and the detection efficiency which is close to 100% with our experimental setup,

$$\sigma_I = \frac{N_d A}{N_i \mathcal{N}_a d \epsilon}. \tag{1}$$

As expected, almost identical values were found for the halo nucleus (^{11}Be or ^{11}Li) and the corresponding core (^{10}Be or ^{9}Li).

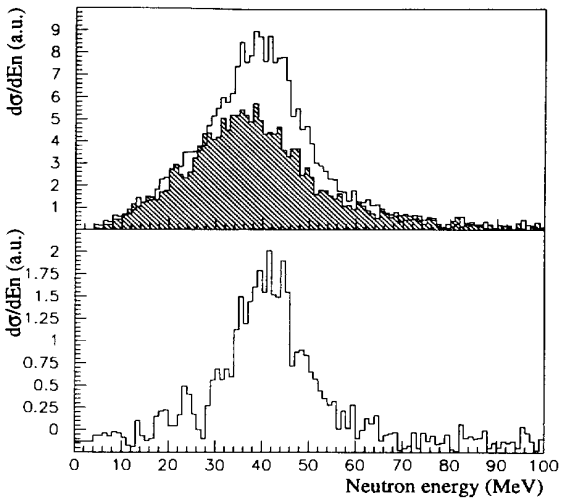

Fig. 3. Neutron energy spectra from ^{11}Be (upper non-filled) and ^{10}Be (upper filled) in coincidence with Li fragments and the subtraction (lower panel).

3.2. Neutrons from the breakup

Neutrons were detected in liquid scintillator-detectors in coincidence with a charged fragment in the telescope. The γ-rays arising from the reactions in the target and the neutrons were clearly separated by using time-of-flight and pulse-shape discrimination. Light charged particles emitted from the breakup reactions (protons, deuterons and tritons), especially at small angles, were also detected in the neutron detectors. In contrast to neutrons, these particles are subject to an energy-dependent, well-defined energy loss in the air and the detector. Thus, they were clearly identified in a two-dimensional plot *deposited energy* vs. *time-of-flight* and removed in the analysis [17].

The efficiency of the neutron detection varies with energy from 34% at 25 MeV to 20% at 70 MeV for the small detectors. The contribution from cross-talk has been estimated by a Monte Carlo simulation and checked by using 14 MeV neutrons [18]. This background was found to be negligible. Finally, a selection in energy of the neutrons was made to eliminate neutrons evaporating from the target in the spectrum shown in Fig. 3. For ^{10,11}Be, a range from 20 to 60 MeV centered around the beam energy in the middle of the target of 38.5 MeV/u, was chosen. In the case of ^{9,11}Li, the selection was extended to 15-60 MeV for a beam energy in the middle of the target of 29.9 MeV/u.

The neutron angular distributions from ^{10,11}Be leading to a Li fragment and the remaining distribution after the subtraction of the ^{10}Be distribution, representing the distribution of the halo neutrons of ^{11}Be, are shown in Fig. 4. The same spectra for a He fragment are shown in Fig. 5, and the spectra of ^{9,11}Li giving a He fragment are displayed in Fig. 6. The insets present the same data on a logarithmic scale. The angular distributions have already been used in many experiments [4,12,16] and the comparison

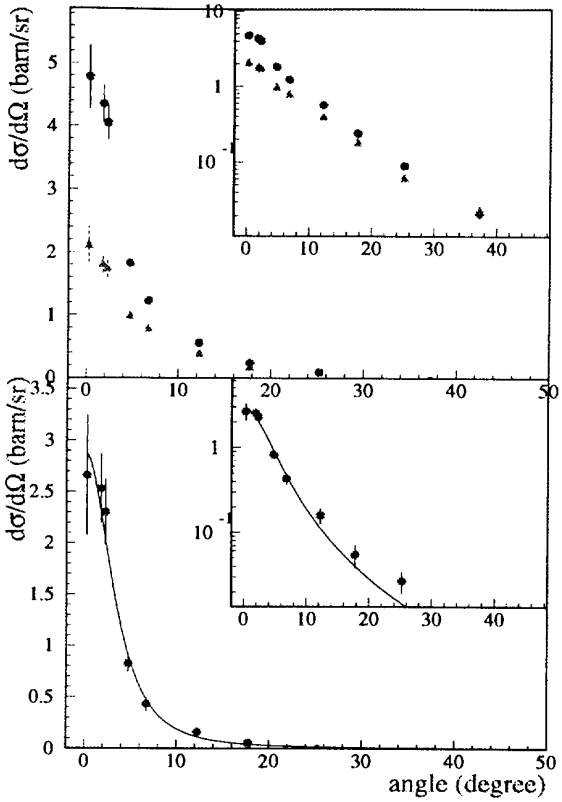

Fig. 4. Angular distributions of the neutrons from ^{11}Be (circles) and ^{10}Be (triangles) in coincidence with a Li fragment (above) and the subtraction of these two spectra, which represents the neutron-halo angular distribution of ^{11}Be in coincidence with a Li fragment (bottom). The full line represents a fit with a Lorentzian shape, giving a width of the distribution of 42±5 MeV/c. The inset presents the same data in logarithmic scale.

with the longitudinal or transverse momentum distributions can be found in [1,5]. The presence of two components is clearly shown in the ^{11}Be and ^{11}Li spectra in the insets (logarithmic scale), a narrow one corresponding to the halo neutrons and a broader one corresponding to the neutrons coming from the core fragmentation. Only the latter is present in the ^{10}Be and ^{9}Li spectra. Note that the broad component has the same magnitude for ^{11}Be and ^{10}Be (and similarly for the Li isotopes), so that subtraction of it leaves only the narrow component from the halo neutrons. This again supports the two-component picture. The full lines represent fits using a Lorentzian shape, Eq. (2), which corresponds to the Fourier transform of a Yukawa wave function, commonly used to describe the halo nucleus [1],

$$\frac{d\sigma_n}{d\Omega} = \frac{\sigma_0 \Gamma}{4\pi(\Gamma^2/4+\theta^2)^{3/2}}. \qquad (2)$$

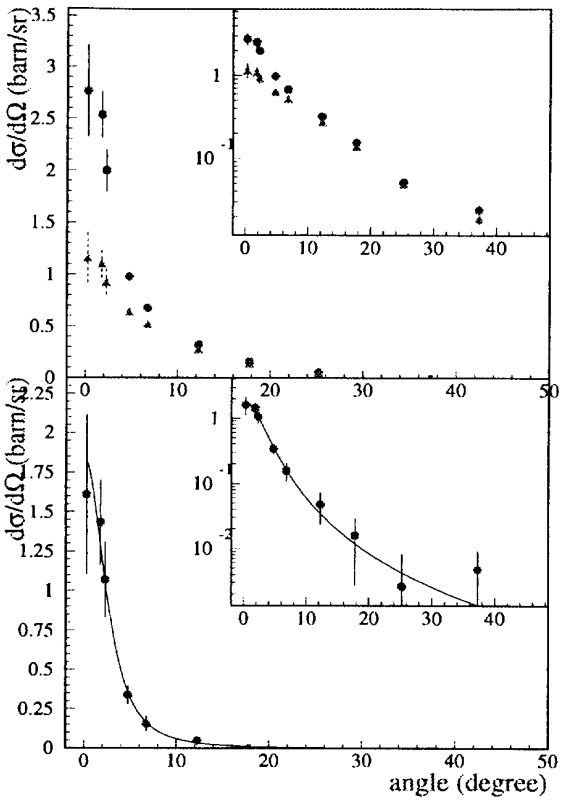

Fig. 5. Angular distributions of the neutrons from ^{11}Be (circles) and ^{10}Be (triangles) in coincidence with a He fragment (above) and the subtraction of these two spectra which represents the neutron-halo distribution of the ^{11}Be in coincidence with a He fragment (bottom). The full line represents a fit with a Lorentzian shape, giving a width of the distribution of 32±5 MeV/c. The inset presents the same data in logarithmic scale.

Table 2
Extracted widths from the neutron halo distribution of ^{11}Be in coincidence with Li or He fragments and from ^{11}Li in coincidence with He fragments

	^{11}Be → Li	^{11}Be → He	^{11}Li → He
Γ(MeV/c)	42±4	32±4	42±6

The widths of the neutron angular distributions are expressed in terms of momentum distribution in Table 2 using the formula $\Gamma(\mathrm{MeV}/c) = \Gamma(\mathrm{radian}) \times p_0$, where p_0 is the beam momentum per nucleon in the middle of the target and σ_0 is the total neutron cross section.

The neutron cross section is obtained by integration of the neutron angular distributions over two different intervals of angles: (0°–21.5°) where the halo effects are

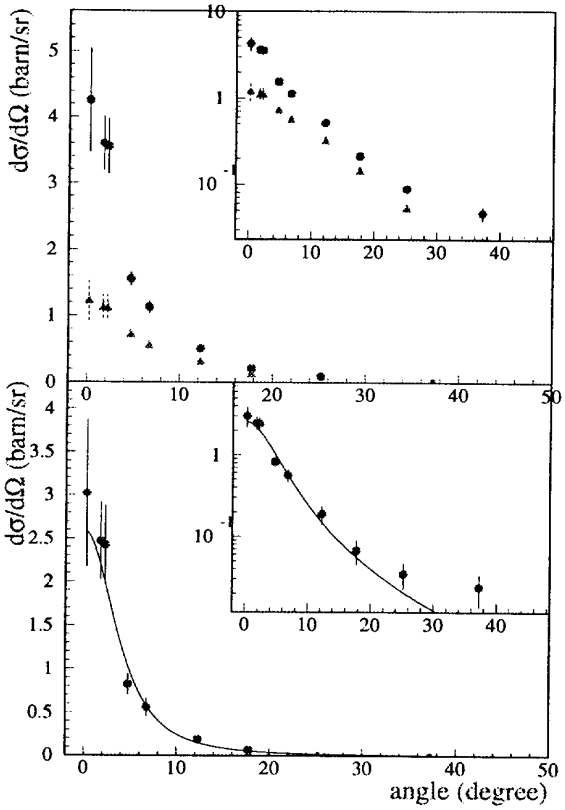

Fig. 6. Angular distributions of the neutrons from ^{11}Li (circles) and ^{9}Li (triangles) in coincidence with a He fragment (above) and the subtraction of these two spectra which represents the neutron-halo distribution of the ^{11}Li in coincidence with a He fragment (bottom). The full line represents a fit with a Lorentzian shape, giving a width of the distribution of 42±6 MeV/c. The inset presents the same data in logarithmic scale.

predominant and in a larger range (0°–53°). The results for the halo nuclei (^{11}Be and ^{11}Li) and the core nuclei (^{10}Be and ^{9}Li) are presented in Table 3 as well as those for the subtracted distributions. We can compare the cross sections from Table 1 and the integrated neutron cross sections from column three (0°–53°) in Table 3 to obtain the halo-neutron multiplicity M_n, Eq. (3).

$$M_n = \frac{(\int (d\sigma_n/d\Omega)\, d\Omega)_{\text{halo}}}{\sigma_r}. \tag{3}$$

The multiplicities are $M_n = 0.33 \pm 0.18$ for ^{11}Be giving a He fragment, $M_n = 0.43 \pm 0.13$ for ^{11}Be giving a Li fragment and $M_n = 0.79 \pm 0.31$ for ^{11}Li giving a He fragment. These values are significantly smaller than the number of halo neutrons, i.e. 1 and 2, respectively. As we shall argue quantitatively below, this is due to the shadow effect when either the target or the core nucleus screen the halo neutrons. Qualitatively, the

Table 3
Integrated neutron cross sections for two different angular ranges for the halo and core nuclei and for the halo component

Angles	$\int(d\sigma_n/d\Omega)d\Omega$ (mb)		
	^{11}Be → Li	^{10}Be → Li	^{11}Be$_{halo}$ → Li
(0°–21.5°)	264±13	169±9	95±16
(0°–53°)	322±19	216±14	106±21
	^{11}Be → He	^{10}Be → He	^{11}Be$_{halo}$ → He
(0°–21.5°)	150±9	113±8	36±12
(0°–53°)	192±14	151±12	41±17
	^{11}Li → He	^{9}Li → He	^{11}Li$_{halo}$ → He
(0°–21.5°)	235±20	128±11	108±23
(0°–53°)	312±32	170±18	142±36

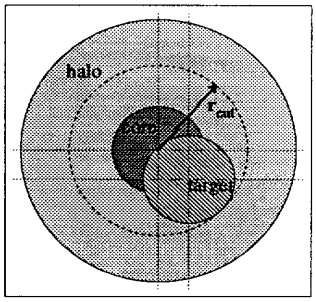

Fig. 7. The core-breakup reaction projected in the plane perpendicular to the beam axis. The target overlaps with the core leading to a reaction zone estimated by the quadrature of the core and target radii.

magnitude of the decrease in M_n reflects that the neutrons even in well-established halo nuclei like ^{11}Be and ^{11}Li have a sizeable overlap with the core. A description of the reaction zone is shown in Fig. 7 in which the charged fragment is formed at an impact parameter smaller than the sum of the core and the target radii. It is clear that in some cases, the halo neutron cannot be transparent to the reaction. By the way, the shadowing of the halo neutron should definitively be considered.

4. Interpretation and discussion

Let us first compare the present widths, Table 2, with results obtained in previous experiments (collected in Table I in Ref. [5]). We note first that an independent measurement of the core component only took place in a single case, ^{11}Li at 28 MeV/u on a Be target. Still, the final average for ^{11}Li of 41±4 MeV/c fits nicely with our

value of 42±6 MeV/c. The values for ^{11}Be differ quite drastically. The final value in [5] of 60±5 MeV/c is substantially larger than our two values of 42±4 MeV/c and 32±4 MeV/c. We tentatively attribute this to the fact that core components were not separated previously. Since our two present values are themselves somewhat different we checked whether the two angular distributions could stem from the same distribution (as in Section 11.5.3 in Ref. [19]). The two agreed, giving a χ^2 of 2.4 for 7 degrees of freedom, but we should nevertheless consider if FSI effects might enter as well. The width in coincidence with Li fragments might have been narrowed due to FSI with a ^{9}Li fragment [5,8], but since previously observed FSI effects with a ^{6}He fragment [20] gave widths around 50 MeV/c and ^{4}He fragments are likely to give even larger widths we cannot explain the data alone via interactions in the final state. Moreover, by comparing the reaction and integrated neutron cross sections, the contribution of ^{9}Li in the Li fragments is estimated to be small. Detailed theoretical calculations are probably needed to reveal the exact influence of FSI, we shall assume in the following that it at most modifies the data slightly.

We then look at the shadow effects to verify that the modifications induced by the core-breakup reactions on the neutron momentum distribution are small. The shadow effects can be understood as a removal of the central part of the halo wave function in the core-target collision. The main expected effect, in addition to a decrease of the neutron multiplicity, is a reduction of the width of the neutron momentum distribution. Indeed, the removal of the central part of the wave function correspond, by Fourier transform, to a cut in the highest component of the momentum distribution. Fig. 8 shows the results of calculations for the halo neutron angular distribution without shadowing (full line) and for several estimations of the shadow effect in the halo wave function (dashed lines).

In a simple model of core-breakup with the halo neutron as a spectator, the multiplicity of neutrons moving with close to beam velocity would be exactly unity. As discussed above, the fact that we measure a multiplicity close to 0.4 for ^{11}Be suggests that the neutron has a large probability of being trapped in the reaction zone. This, however, must have consequences also for the measured momentum. It has been shown [9,10] that the experimental longitudinal momentum of the heavy fragment explores certain regions of space with larger probability than others. The regions that are "shadowed" do not contribute, hence the name "shadow effect" for this phenomenon. We have examined the magnitude of this effect on the transverse momentum in a highly schematic model, similar to the one used previously [10]. There is no selection on the exit channel (Li or He fragments), considering only that the core of the halo nucleus has broken up due to an impact parameter smaller than the sum of the core and target radii. In this model of the shadow effect on transverse neutron momentum, we assume that the reaction zone at the centre of the halo turns opaque to the halo neutron and that we are sampling only the peripheral part of the neutron wave function. For simplicity we represent this by the outside of a cylinder with radius r_{cut}, see Fig. 7, and calculate the corresponding content of transverse momentum. This can be expressed in terms of a spatial integral over the two-dimensional Wigner transform. (The longitudinal momentum spectrum [10] involves the one-dimensional Wigner transform in the beam direction. This is free of

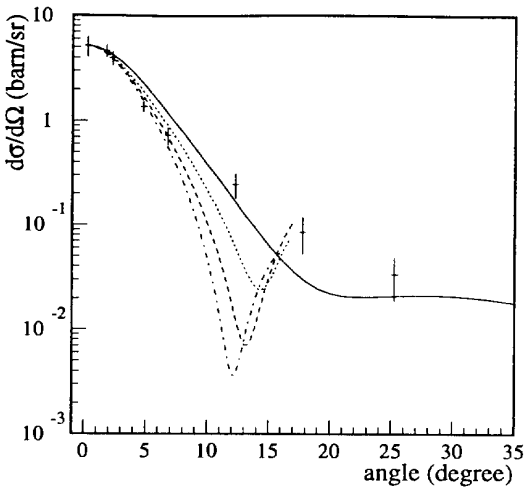

Fig. 8. Comparison of the experimental angular distribution of the halo-neutrons coming from ^{11}Be (without selection on the exit channel considering only that the core has broken up, i.e. $Z \leqslant 3$), the calculated distributions without shadowing (full line) and with three different cutoff radii for the halo wave function (3, 3.86 and 4.5 fm for the dotted, dashed and dot-dashed lines, respectively).

diffractive effects, which is not the case here). For clarity, some main results of this calculation will be given in the following.

Assuming that the $1s_{1/2}$ dominates the ^{11}Be ground state, the total single-particle wave function for the halo without shadow effects was calculated with a Woods–Saxon potential with radius and diffuseness parameters $r_0 = 1.25$ fm and $a = 0.7$ fm. The well depth was adjusted to reproduce the experimental separation energy of ^{11}Be ($S_n = 0.504$ keV). The corresponding angular distribution is shown as a full line in Fig. 8. For angles smaller than 10° where the halo effects are dominant, the calculated amplitude of the distribution is larger than the experimental one whereas, for angles larger than 20°, the nearly constant amplitude is associated with the inner part of the s-wave wave function. For angles greater than 12°, the calculated amplitude is somewhat smaller than the experimental one, but the difference could be due to the procedure of subtraction of the core component. Indeed, this procedure is not able to remove the halo neutrons scattered in the collision with the target and detected at relatively large angles.

The shadow effect implies a cylindrical geometry, shown in Fig. 7. It is therefore convenient instead of the angular distribution to calculate the distribution on transverse momentum $k_\perp = k_0\theta$ in the form of the integral

$$\frac{dW}{d\varphi k_\perp dk_\perp} = \int_{-\infty}^{+\infty} |A(k_\perp, \varphi_k, z)|^2 dz, \tag{4}$$

where k_0 is the beam momentum. To calculate the amplitude $A(\boldsymbol{k})$, it is assumed that the neutron will only be detected if it is outside of the reaction zone approximated by a

perpendicular cutoff radius ($r_\perp > r_{\rm cut}$). Since this is always larger than the core radius, the exact wave function $\Psi(\boldsymbol{r})$ is simply the first spherical Hankel function, defined as

$$\Psi_0(r) = \begin{cases} B\kappa^{3/2} h_l(i\kappa r)\, Y_{lm}(\theta,\varphi) & \text{for } r_\perp > r_{\rm cut}, \\ 0 & \text{elsewhere.} \end{cases} \tag{5}$$

written in terms of the reduced mass (μ) and the neutron separation energy (S_n) through the relation $\kappa = (2\mu S_n)^{1/2}/\hbar$. The magnitude of the effective cutoff radius can be estimated very roughly from the core and target radii in such a way that the area blocked in the reaction is, at most, the sum of the core and target projected areas. For a first estimate of the shadow effect, this leads to estimate that cutoff radius as the quadratic sum of the core and target radii $r_{\rm cut} = \sqrt{r_c^2 + r_t^2}$ and is therefore equal to 3.86 fm for ^{11}Be on a Be target. Then, the amplitude $A(\boldsymbol{k})$ is given by

$$A(k_\perp, \varphi_k, z) = -\frac{B}{\sqrt{4\pi\kappa}} \int_{\sqrt{(\kappa z)^2 + (\kappa r_{\rm cut})^2}}^{+\infty} J_0\left(\frac{k_\perp}{\kappa}\sqrt{(v^2 - \kappa z)^2}\right) e^{-v} dv. \tag{6}$$

The constant B is determined by joining the outer and the inner solutions of the Schrödinger equation. For the WS potential used before, a value of $B = 2.26$ is found for ^{11}Be while a Yukawa wave function gives $B = \sqrt{2}$ for an $l = 0$ state, sometimes augmented by a finite size correction [4]. The angular distributions corresponding to a shadowing with respectively a 3.0, 3.86 and 4.5 fm cutoff are shown in Fig. 8 (dashed lines). By comparison with the WS calculation (full line), one observes, as expected, a decrease of the width for angles smaller than 12° where the calculated distributions agree very well with the experimental one. For angles larger than 12°, the nearly constant amplitude disappear corresponding to the fact that the shadow effects completely remove the central part of the halo wave function. The sharp increase could be connected to the diffraction of the halo neutron but the calculations are too schematic to justify a quantitative comparison.

One should note that the about 10% change in width for ^{11}Be due to shadowing is clearly smaller than that seen for ^{8}B [9–11], this is due to ^{11}Be being a reasonable well-developed halo. Still this halo is overlapping noticeably with the core as shown by the experimental value for the halo-neutron multiplicity in the core-breakup channel ($M_n = 0.38 \pm 0.09$) that should be compared to the multiplicity given by the model. The cutoff radii at 3.0, 3.86 and 4.5 fm give multiplicities of 0.58, 0.41 and 0.30, respectively. This range overlaps nicely with the experimental value.

Since ^{11}Be is a one-neutron halo nucleus the widths of the momentum distributions extracted from the core data in dissociation reactions and for the neutron distributions in core-breakup reactions should be the same ($\Gamma_{\rm core}/\Gamma_{\rm neutron} = 1$) if no reaction mechanisms are involved. Both sets of data will be affected slightly by shadowing as discussed above, but the average value from the core momentum distributions of $\Gamma = 47 \pm 7$ MeV/c [17,21] already agrees both with our values and with the recent theoretical predictions [9,10]. These give an intrinsic width of about 46 MeV/c, and when shadowing is included of 40–41 MeV/c.

In the case of ^{11}Li, the interpretation is somewhat different since ^{11}Li is a two-neutron halo nucleus. The value of $\Gamma = 42 \pm 6$ MeV/c obtained in coincidence with He fragments is in complete agreement with both parallel momentum distributions of the core (Γ of 47±6 MeV/c [17,21]) and previous measurements of the neutron momentum distributions (Γ of 41±4 MeV/c [5]). We know that FSI can play an important role in the dissociation of ^{11}Li but in the core-breakup reactions used here the impact might be reduced. Indeed, the same width ($\Gamma = 41 \pm 6$ MeV/c) is found when a selection including not only the He fragments but all the $Z \leqslant 2$ charged fragments is performed. The shadow effect discussed for ^{11}Be will also appear for ^{11}Li as seen by the neutron multiplicity that is reduced from 2 to $M_n = 0.79 \pm 0.31$. The effect on the width of the momentum distribution require a more complete model treating the n–n correlations, such calculations with inclusion of shadowing are only now starting to be developed [22,23].

5. Conclusions

The neutron momentum distributions in core-breakup reactions were measured for ^{11}Be and ^{11}Li with a proper background subtraction of the neutrons arising from the core fragmentation. The width $\Gamma = 42 \pm 6$ MeV/c for ^{11}Li in coincidence with He fragments is in perfect agreement with previous measurements and with measurements of parallel momentum distributions of the core ^{9}Li. Widths of $\Gamma = 42 \pm 4$ MeV/c and $\Gamma = 32 \pm 4$ MeV/c have been extracted for ^{11}Be in coincidence with Li and He fragments. This result differs from the previous measurement showing clearly the importance of a precise background subtraction and the necessity of the highest selectivity possible in the exit channel. Taking into account the shadowing, which leads to a 10% decrease of the experimental width, this result is in very good agreement with the parallel momentum distributions of the core ^{10}Be. This is the first time that both halo-neutrons and core distributions are in agreement and compatible with recent theoretical predictions of approximately 46 MeV/c. Furthermore, the rather low neutron multiplicity for ^{11}Be was measured for the first time and interpreted as due to the core-target shadowing. We have presented a simple model where the main ingredients are included, but a more sophisticated analysis including integration over the impact parameter is needed for a more profound understanding.

In conclusion, the core-breakup reactions can be used for detailed studies of neutron halo structures. For future work it is important, apart from doing a proper subtraction of neutrons from the core fragmentation, to be selective regarding the isotope identification in the final state in order to identify possible FSI or other effects like an impact parameter dependence.

Acknowledgements

We thank the technical staff of LISE3/GANIL for their help during the experiment. We are also indebted to the NORDBALL collaboration for the use of their neutron detectors. Finally, we have benefited from fruitful discussions with M. V. Zhukov.

References

[1] P.G. Hansen, A.S. Jensen and B. Jonson, Ann. Rev. Nucl. Part. Sci. 45 (1995) 591.
[2] I. Tanihata, J. Phys. G 22 (1996) 157.
[3] B. Jonson and K. Riisager, Phil. Trans. R. Soc. Lond. A 356 (1998) 2063.
[4] R. Anne et al., Nucl. Phys. A 575 (1994) 125.
[5] T. Nilsson et al., Europhys. Lett. 30 (1995) 19.
[6] T. Kobayashi, in Proc. Third Int. Conf. on Radioactive Nuclear Beams, ed. D.J. Morrissey (Editions Frontières, Gif-sur-Yvette, 1993) p. 169.
[7] F. Barranco, E. Vigezzi, R.A. Broglia, Phys. Lett. B 319 (1993) 387.
[8] M. Zinser et al., Phys. Rev. Lett. 75 (1995) 1719.
[9] H. Esbensen, Phys. Rev. C 53 (1996) 2007.
[10] P.G. Hansen, Phys. Rev. Lett. 77 (1996) 1016.
[11] M.H. Smedberg et al., submitted to Phys. Lett.
[12] M. Marqués et al., Phys. Lett. B 381 (1996) 407.
[13] D. Bazin et al., Phys. Rev. C 57 (1998) 2156.
[14] T. Baumann et al., Phys. Lett. B 439 (1998) 256.
[15] A.C. Mueller and R. Anne, Nucl. Inst. Meth. B 56 (1991) 559.
[16] R. Anne et al., Phys. Lett. B 304 (1993) 55.
[17] S. Grévy, PhD, University of Paris XI, France (1997), IPNO-97-24.
[18] M. Cronqvist et al., Phys. Lett. A 317 (1992) 273.
[19] W.T. Eadie et al., Statistical methods in experimental physics (North-Holland, Amsterdam, 1971).
[20] T. Nilsson et al., Nucl. Phys. A 598 (1996) 418.
[21] N. Orr, Nucl. Phys. A 616 (1997) 155c.
[22] G.F. Bertsch, K. Hencken and H. Esbensen, Phys. Rev. C 57 (1998) 1366.
[23] E. Garrido, D.V. Fedorov and A.S. Jensen, Europhys. Lett. 43 (1998) 386.